TRANSPORT OF SURFACTANTS IN FRACTURED CHALK ROCK – LABORATORY EXPERIMENTS AND NUMERICAL SIMULATIONS

Ingebret Fjelde[1], John Fabricius Zuta[2] and Ann Helen Kvæstad[3]
[1]International Research Institute of Stavanger (IRIS)
[2]Geological Survey of Denmark and Greenland (GEUS)
[3]Norwegian Petroleum Directorate (NPD)

This paper was prepared for presentation at the International Symposium of the Society of Core Analysts held in Aberdeen, Scotland, UK, 27-30 August, 2012.

ABSTRACT

Surfactants can be used in different types of enhanced oil recovery (EOR) processes, such as the stabilization of foam to improve the macroscopic sweep efficiency in gas floods, reduction of the interfacial tension to reduce the residual oil saturation, and wettability alteration to improve the spontaneous imbibition of water in fractured reservoirs. In fractured reservoirs, the retention of the surfactants will depend on how much of the matrix is contacted by the surfactant during the project period. In presented study, knowledge about transport of surfactants in fractured chalk has been established in laboratory experiments and simulations.

Chalk plugs at 100% water-saturation and residual oil saturation after water flooding were used in the static experiments. Fractured models were created by placing core plugs in cells with an annulus space around the plugs. The fracture volume was filled with the surfactant solution. In addition to fractured models with all surface area of the plugs exposed to the surfactant solution, different fractured models were created by blocking some of the surface area for surfactant exposure. Water samples were regularly taken out from the fracture and analyzed for the surfactant concentration until the concentrations reached a plateau.

It was observed that increasing the exposed surface area or decreasing the maximum transport length increased the rate of retention. The presence of an immobile oil phase did not have large effects on the total retention of the surfactant. The experiments were also modeled with the commercial reservoir simulator STARS. Excellent history-matching of the surfactant concentration profiles was obtained for the plugs with all surface area exposed. The same dataset was used to predict the surfactant concentration profiles for the fractured models with different surfaces blocked. Simulation studies at larger scale show that the whole matrix blocks will not be saturated with the surfactant during typical time for EOR-processes. The retention of surfactants will therefore be much lower in fractured reservoirs with diffusion dominated transport of surfactants from fractures to matrix than estimated based on flow through experiments. The amount of surfactant required for EOR-processes mainly affecting the flow in the fractures and/or close to the fractures, will for this reason be less than required for saturation of the whole matrix. For EOR-processes where transport of the surfactant into most of the matrix is required, the potential will be low in these reservoirs because the transport of surfactant in the matrix will be too slow.

INTRODUCTION

A considerable portion of the world's hydrocarbon reserves can be found in carbonate reservoirs (Akbar et al. 2000), and these are mostly fractured (Manrique et al. 2007). North Sea chalk reservoirs are examples of naturally fractured reservoirs where the matrix blocks

are characterized by very high porosity and low permeability (Allan and Sun, 2003). The wettability of carbonate reservoirs is generally regarded as mixed-wet or oil-wet (Chilinger and Yen, 1983). The North Sea chalk reservoirs are rather water-wet (Hamon, 2004). This means that the oil recovery from water flooding of fractured carbonates reservoirs can be low due to poor spontaneous imbibition of water into the matrix blocks.
Gravity drainage can be an important recovery mechanism if the formation is highly fractured and the permeability of the fracture is greater than the permeability of the matrix ($k_f >> k_m$). Miscible gas injection (Darvish et al. 2006; Morel et al. 1993) and chemical treatment (Adibhatla and Mohanty, 2008) can be used to recover oil from highly fractured carbonate reservoirs. In chemical EOR, different classes of surfactant solutions can be injected into fractured carbonate reservoirs with the aim of changing the wettability of the matrix to a water-wet state, hence enhancing the spontaneous imbibition process. Standnes and Austad (2000) observed that in oil-wet chalk plugs, both cationic and anionic surfactants can alter the rock wettability towards a more water state. Laboratory experiments have demonstrated that CO_2 at elevated pressures can recover significant amounts of oil in fractured reservoirs (Darvish et al. 2006). However, a problem in CO_2 flooding is the low viscosity of CO_2 and thereby the high mobility of CO_2 compared to the crude oil. CO_2-foam has been found to increase the apparent viscosity of CO_2 and improve the oil recovery in fractured chalk reservoirs (Zuta et al. 2009; Zuta et al. 2010a). In these EOR processes, the transport of the EOR agent from the fracture into the matrix is important in the fractured chalk reservoirs. For significant wettability alteration to occur in fractured chalk reservoirs, the surfactant solution needs to be transported from the fracture into the matrix at sufficient concentrations. In fractured chalk reservoirs with low permeability, the success of a CO_2-foam process will depend on the transport of CO_2 from the fracture to the matrix. This will require that the injected foam-forming surfactant solution provides enough mobility control to improve the macroscopic sweep efficiency in a fracture network. However, transport of the foam-forming surfactant from the fracture network into the matrix blocks can retard the process and eventually the oil recovery process.
In this paper laboratory experiments have been used to study the transport of an anionic surfactant in fractured chalk models. Different fractured models were created and used. The effect of oil on the transport of the surfactant solution was also studied. The experiments were modelled with a commercial reservoir simulator STARS. Additional simulations were performed in hypothetical large simplified matrix blocks.

EXPERIMENTAL PROCEDURES

Porous media

Core plugs from an outcrop of Liege chalk with a minor amount of clay and less than 2wt% silica (Strand et al. 2007), were used for all of the experiments. The plugs were sampled from the same block. All the plugs had a diameter of 3.8 cm and a length of approximately 7.0 cm.

Chemicals and fluids

Synthetic seawater (SW) and formation water (FW) with the compositions as shown in **Table 1**, were filtered (0.45 μm) before use. The surfactant used was an anionic surfactant, branched ethoxylated sulphonate (BES) with 3-12 carbon atoms in its chain length and 6 ethylene (EO) groups. Surfactant solutions (0.86wt%) were prepared with SW. Stock tank oil (STO) from a North Sea reservoir was used, and was filtered online at 90ºC during for core preparation.

Preparation of plugs with formation water
The plugs were stored at 120ºC until they reached constant weights before they were saturated with FW. Since sulphate is found in Liège outcrop and this can change the wettability to water-wet during aging with crude oil (Fjelde, 2008), the 100% FW saturated plugs were cleaned of sulphate by flooding them with FW no sulphate was detected in the effluent samples. The absolute permeability (k_{abs}) of the plugs to FW was also measured (**Table 3**).

Preparation of plugs with stock tank oil
Plugs with initial water saturations (S_{wi}) were established by draining 100% FW saturated plugs with humidified N_2 gas at room temperature with the unconfined porous disc method by gradually increasing the pressure to 15 bar. The plugs were later aged with continuous injection (in opposite directions) of stock tank oil (STO) at 0.08 ml/min at 90ºC for 80 hours. Similar preparation of reservoir chalks has given Amott index of approximately 0.6. The core plugs were water flooded with SW at injection rates of 0.1, 0.2 and 0.5 ml/min until there was no more oil produced.

Preparation of fractured chalk models
The experiments were carried out in fractured chalk models (Figure 1). Core plugs were placed into plastic containers with an inside diameter of 5.2 cm. This created a 1.4 cm, or 0.7 cm x 2, annulus space around the core plug, between the core plug and the wall of the container. This annulus space created an artificial fracture. Glass beads were placed at the bottom to enable the transportation of the surfactant solution to occur on all the surface areas. The core plugs used were at 100 % water saturation (S_w=100%) or at residual oil saturation after water flooding (S_{orw}). Figure 2 shows the five (5) different designs that were used in the experiments. Teflon-tape and shrinkable-teflon were used to block the different surface areas of the core plugs.

Procedure for static experiments
The static experiments (with no viscous displacement) were carried out by filling the annulus volume (approx. 133 ml) around the plugs with 0.86 wt% (active) surfactant solution. The experiments were carried at 55ºC and atmospheric pressure. The experiments were carried out in parallels with liquid samples (1.5 ml) periodically taken out from the space above the plugs and analyzed until the concentrations reached a plateau. It was assumed such an intrusion will have a negligible effect of the measured surfactant concentration.

Analytical methods
Sulphate analyses were done using a sulphate cell test kit (Spectroquant 1.14548.001) (ASTM D516-07). Surfactants in effluent samples were analyzed by a two phase titration method using Hyamine, a cationic surfactant. The analyses were performed using the cationic dye methylene blue as indicator and chloroform as organic phase (Schmitt, 2001).

RESULTS AND DISCUSSION
The physical properties of the fluids interfacial tensions (IFT), density, viscosity, and pH are listed in **Table 2.** The interfacial tension was not ultralow, because a foam forming surfactant was used.
Plugs with similar properties were selected for the experiments (**Tables 3 and 4)**. The porosity of the plugs varied between 39.8- 43.1 %, while the absolute permeability (k_{abs}) to

FW ranged between 0.63 – 1.87 mD. In the presence of oil, S_{orw} in the plugs ranged between 23.9-30.4% after water flooding. Two-phase production after the water breakthrough was observed in these water floods, and the end point permeability at S_{wi} and S_{orw} were rather similar. This indicated rather mixed-wet core plugs.

The static experiments in the fractured models were carried out over a period of approximately 60 days. Figures 3-5 show the surfactant concentration in the fracture as a function of time for the different designs. In all cases, the surfactant concentration in the fracture decreased with time. The transport of the surfactant was expected to occur because of adsorption and molecular diffusion of the surfactant from the fracture into the matrix. However, the transport of the surfactant from the fracture to the matrix was expected to depend on the different designs. Figure 3a shows the results for the base case fractured model at S_w=100%. In this design, all the surface areas of the plugs were open and exposed to the surfactant solution (Figure 2a). The surfactant was transported from the fracture into the core plugs from all sides. As shown in Figure 3a, the surfactant concentration declined very rapidly during the first 8 – 10 days, and stabilized after 10 days at a concentration of approximately 0.45 wt% in the fracture. It was estimated that 40-50% of the reduction in concentration was due to dilution of surfactant solution with the brine in the core plugs. The constant concentration indicated that equilibrium had been achieved. As shown in Figure 3a, the two parallel core plugs had similar surfactant concentrations throughout the experiments.

The experiments with the lateral surface area blocked are shown in Figure 3b. In this case, the surfactant was transported into the core plug through the top and bottom exposed surface areas (see Figure 2b). The figure also shows a similar experiment with a core plug (FB30) at S_{orw}. The surfactant concentration in both cases decreased fast within the first 10 – 12 days, and then the reduction was much slower. The parallel core plugs with S_w=100% (AH25 and A26) had similar surfactant concentration throughout the experiments. The concentration at the end of the experiments was approximately 0.51 wt%. Compared with the base case at S_w=100%, it is seen that the plugs had not reached equilibrium surfactant concentration. The concentrations were expected to continue to decrease until it had reached an equilibrium concentration of approximately 0.45 wt%. The core plug at S_{orw} (FB30) followed the same trend as the core plugs at S_w=100%. The difference was that the concentration in the fracture at S_{orw} was slightly higher than for the core plugs at S_w=100%. This might be due to less accessible pore volume in the core plug at S_{orw}. Since the core plugs with oil appear to be mixed-wet, oil components might have occupied some of the surface area in the chalk where the surfactant could have been retained. The concentration at the end of the experiments for the plug at S_{orw} was 0.57 wt%.

Figure 4a shows the experiments in which the top and lateral surfaces of the plugs were blocked (See Figure 2c). In this design, the transport of the surfactant occurred at the bottom-exposed area. The surfactant concentrations in the fracture for the two parallel core plugs, A29 and A31, were similar during the experiments. As shown in Figure 4a, the concentration decreased fast to 0.75 wt%, and then decreases more slowly. The concentration at the end of the experiments was 0.60 wt%. Thus, equilibrium concentration has not been reached compared to base case, and the concentration is expected to continue to decrease until it reaches the equilibrium concentration.

In Figure 4b the top surface area was exposed to the surfactant solution (Figure 2d). There was not much difference between the core plugs at S_w=100%, A32 and A33, and the core plug at S_{orw}, FB29. Fast reduction in surfactant concentration occurred in the beginning before it was gradually decreased within the next 30 days, afterwards, the concentration decreased very slowly. As shown in Figure 4b, the two parallel cores (A32 and A33) at S_w=100% started to differ slightly around 30 days. This might be due to the varying degree

of heterogeneity in the plugs - permeability difference between the core plugs. The average concentration at the end for the core plugs at S_w=100% was 0.60 wt%. The equilibrium concentration had not been reached for this design compared to the base case at S_w=100% in Figure 3a. The concentration profile for the core plugs at S_w=100% and the core plug at S_{orw} had the same trend, and there was only a small difference in concentration between them. The concentration at the end for the core plug at S_{orw} was 0.62 wt%.
Figure 5 shows the experiments in which half of the lateral surface and the bottom of the plugs were wrapped in Teflon and not exposed to the surfactant solution (Figure 2e). The transport of the surfactant was expected to occur through the half of the top lateral surface area and the top surface area as shown in Figure 2e. The surfactant concentration (in the fractures) as a function of time in the two parallel core plugs, A27 and A28, were similar. As shown in Figure 5, the concentration decreased mainly within 15 - 20 days, and. The concentration at the end of the experiments was 0.52 wt%. Compared to the base case (Figure 3a), the equilibrium concentration had not been reached at approximately 55 days.

Mechanistic modeling of static experiments
Numerical simulations of the static experiments were performed with the Computer Modelling Group's (CMG) commercial reservoir simulator STARS. The laboratory core plugs with constant diameters of 3.8 cm and a length of approximately 7.0 cm were represented by a radial model with 50*1*100 grid blocks. The same grid model was used to represent both the rock and the fracture. Figure 6 shows the physical grid blocks including the fracture and matrix established in STARS. The 41*1*96 (3.8 cm diameter plug) portion of the rock grid blocks were given petrophyscial properties similar to the plugs. The remaining non-rock grid blocks were assigned properties representing the fracture. The fracture was assumed to be of infinite permeability and was always filled with the surfactant solution. A porosity of 0.99 and a permeability of 1000 mD were assigned to the fracture. The plugs were either at S_w=100% or S_{orw}.
In the simulation study, the transport of the surfactant was assumed to occur by only adsorption and diffusion of the surfactant from the fracture into the rock. It was assumed that there will be no adsorption on the fracture walls because the external surface are of the core plugs was small compared to the surface area inside the core plugs. The simulations in the different designs (Figure 2) were created by setting the transmissibility to zero on the surface areas that were blocked. The surfactant concentration in the fracture was monitored over time for the different designs. It was decided to take samples over the core plug. In STARS the maximum adsorption level (ADMAXT) and residual adsorption level (ARDT) can be made region dependent, so that these properties can vary from grid block to grid block (CMG manual, 2008). The adsorption of the surfactant onto the rock was modelled by a Langmuir static adsorption isotherm (Figure 7) determined on crushed Liege rock at room temperature and 55ºC. The ratio of crushed rock to the surfactant solution was 1:3.
The adsorption of the surfactant onto Liege rock increased with increasing equilibrium surfactant concentration. However, as shown in Figure 7, the adsorption was higher at room temperature (RT) than at 55ºC. Increasing the temperature is generally believed to increase the solubility of the surfactant and decrease the adsorption of the surfactant molecules. The rock and fracture parameters used at 55ºC in STARS (CMG manual, 2008) are as defined in **Table 5 and 6**.
In the simulations, the base case experiments - fractured model where all the surface areas were exposed to the surfactant solution at S_w=100% (Figure 2a) were first history-matched. This was done by tuning the effective diffusion coefficient (D_{eff}) of the surfactant in the fracture. The other experiments (Figures 8b-10) were predicted using the same data as used for the base case experiments. The only parameter that was changed in the predictions was

the transmissibility on the surface area that was blocked. As shown in Figure 8a, the experimental results (Figure 3a) were successfully history-matched with an effective diffusion coefficient of $3*10^{-5}$ cm^2/min. Thus, there was a good agreement between the experimental results and the history-match. Rossen (2004) reported an apparent diffusion coefficient (D_{app}) for surfactants in water to be in the region of $1*10^{-6}$ cm^2/min at room temperature. In Figure 8b, the same data set were used to predict the experimental results (Figure 3b) in the fractured model with lateral surface areas of the plugs blocked.

Although there was a slight deviation in the predicted concentration profile the first 0-30 days, the predicted profile matched well with the experimental results after 30 days. However, the slight deviation within 0-30 days was within an experimental error of ± 5.0%. Figure 9a shows the predicted versus experimental results (Figure 4a) at S_w=100%. In this case, the fractured model involved plugs with all the surface areas blocked except the bottom opened to the surfactant solution. The predicted result from the simulations showed an approximately 6 – 14 % higher surfactant concentrations than measured in the experimental results. However, the trend of the prediction was similar to the experimental results. Figure 9b also shows the prediction of the experimental results for fractured model with the lateral surface area and bottom blocked at S_w=100%. Although the trend of the prediction was similar to the experimental results, the prediction was approximately 6 – 14 % higher than the experimental results.

The predicted results for the case where half the lateral surface area and bottom is blocked at S_w=100% is shown in Figure 10. The same data set were used to predict the experimental results. As shown in Figure 10, there was a good agreement between the experimental and the predicted results.

Figure 11 shows the experimental results and different history-matches for the core plug at S_{orw} with the lateral surface area and bottom blocked. The S_{orw} for plug FB29 was determined as 30.4 % (see Table 4). The effective diffusion coefficient at S_{orw} is dependent on both the diffusion coefficient of the surfactant in water and oil phases. However, since the diffusion coefficient for surfactant solution in oil phase was not known, the effective diffusion coefficient for the surfactant solution was estimated based on the effective diffusion of the surfactant in the water phase and residual water saturation ($1-S_{orw}$), i.e. $D_{eff} = D_w S_w + D_o S_o$. The history-matches were done with two different maximum adsorption capacity (ADMAXT) in the matrix. In this first case the ADMAXT in the matrix was set equal to the ADMAXT measured at S_w=100%. The second case involved an ADMAXT 100 times larger than measured at S_w=100%. The reason why a higher ADMAXT in the matrix was tried was because flow-through retention experiment not reported here showed that the retention was higher at S_{orw} (Kvæstad, 2011). The rock and fracture input parameters that were used are shown in Table 5. In Figure 11, an effective diffusion coefficient of $2.1*10^{-5}$ cm^2/min and a ADMAXT of $1.26*10^{-3}$ gmol/cm^3 was used to history-matched the experimental results. This is an adsorption that is 100 times larger than in the case at 100 % water saturation. No partitioning of the surfactant into the oil phase was observed.

The trend of the history-match is similar to the experimental results. The history-match with b = 4, predicted too high surfactant concentration remaining in the fracture when compared to the experimental results. Figure 11 shows the experimental results and different history-matches for the core plug at S_{orw} with the lateral surface area blocked. The S_{orw} for FB30 was estimated as 24 %. An effective diffusion coefficient of $2.3 \cdot 10^{-5}$ cm^2/min was used. The best history-match for this design was with b = 4. This means that the ADMAXT in the matrix was $1.26*10^{-4}$ mol/cm^3. This is an adsorption that is 10 times larger than in the cases at 100 % water saturation. This trend of the history-match is similar to the experimental results.

Mechanistic Modeling of static experiments in large blocks

Additional simulations were performed to investigate the transport of the surfactant solution in large matrix blocks similar to Figure 2d (lateral surface and bottom blocked) at S_w=100%. This design was chosen because it could be compared with the surfactant solution been transported from the fracture and into one side of the matrix block in the reservoir. The same data set used in predicting the experimental results in Figure 9b were used. The blocks had a constant diameter of 30 cm and the ranged between 30 – 70 cm. The transport of the surfactant solution was simulated for 5 000 days. The simulations were performed to see if the equilibrium concentrations would be reached during 5 000 days and to determine how the length of the blocks will affected the rate of retention. In Figure 12 the change in surfactant concentration in the fracture vs. time is plotted. In Figure 12 it is seen that all three cases show a fast decline in surfactant concentration in the fracture during the first few days, and then the decline is more slowly. The rate of retention was highest in the core plug with dimensions 30cm x 30cm, and it was lowest in the core plug with dimension 30cm x 70cm. The equilibrium concentration was not reached after 5 000 days. From Figure 12 it is seen that the concentration will reach equilibrium first in the block with the shortest length. Earlier performed simulation on large scale with a constant diameter also showed that the transport of foam-forming surfactant would depend on the heights of the matrix blocks (Zuta et al. 2010b). If the transport of the surfactant in the fractured reservoirs is dominated by diffusion, the transport will be too slow for EOR-processes that should affect the flow conditions in the matrix blocks, e.g. wettability alteration. For EOR-processes mainly affecting the flow in fractures and close to fracture, the slow transport of surfactant into the matrix can be especially beneficial.

CONCLUSIONS

Based on the experimental and simulation results, the following conclusions can be made;

- The transport of the surfactant solution increased with increasing surface area of the core plugs exposed to the surfactant solution.
- The transport of the surfactant solution was determined to depend on the type of surface area blocked. This also influenced the time it took to reach equilibrium concentrations. The reason been that the maximum transport length for the surfactant solution varied.
- The presence of an immobile oil phase at mixed-wet conditions did not have a significant effect on the total surfactant retention.
- A history-match of the base case fractured model at S_w=100 % was performed, and the predictions of the other fractured model designs at 100 % water saturation were in good agreements with the experimental results.
- Additional predictions based on large matrix blocks with lateral surface and bottom blocked showed it will take a long time before the matrix blocks are fully saturated with the surfactant solution.
- The results from the experiments and simulations performed in this work show that the surfactant solution used will have a low retention rate in the field and it may take a long time to saturate the reservoir.

NOMENCLATURE

$ADMAXT$ = maximum adsorption capacity
C = effluent surfactant concentration during flooding, mg/g
C_o = initial concentration of surfactant solution, mg /g
D_{app} = apparent molecular diffusion, cm^2/min
D_{eff} = effective molecular diffusion, cm^2/min
D_w = diffusion coefficient in water phase, cm^2/min
FW = formation water
k_{abs} = absolute permeability to formation water, mD
k_{eff} = effective permeability of fractured model, mD
PV = pore volume, ml
S_{orw} = residual oil saturation after water flooding, % PV
S_{wi} = initial water saturation, % PV
SW = seawater

REFERENCES

Adibhatla, B., and Mohanty, K. K. 2008. Oil Recovery from Fractured Carbonates by Surfactant-Aided Gravity Drainage: Laboratory Experiments and Mechanistic Simulations. *SPE Res Eval & Eng 11* (1): 119-130.SPE 99773-PA.

Akbar, M., Vissapragada, B., Alghamdi, A. H., et al. 2000. A Snapshot of Carbonate Reservoir Evaluation. *Oilfield Review 12* (4): 20-21.

Allan, J., and Sun, Q. 2003. Controls on Recovery Factor in Fractured Reservoirs: Lessons Learned from 100 Fractured Fields. SPE 84590. SPE Annual Technical Conference and Exhibition, Denver, Colorado, 5-8 October.

American Society for Testing and Materials (ASTM). 2007. D156-07. Standard Test Method for Sulphate Ion in Water.

Chilingar, G.V. and Yen, T.F. 1983. Some Notes on Wettability and Relative Permeability of Carbonate Rocks. II. *Energy and Sources 7* (1): 67-75.

CMG Manual. 2008. Computer Modeling Group. Component Adsorption and Blockage in Appendix D7: Fluid and Rock properties.

Darvish, G.R., Lindeberg, E., Holt, T., Utne, S.A., and Kleppe, J. 2006. Laboratory Experiments of Tertiary CO_2 Injection into Fractured Cores. Paper SPE 99649. SPE/DOE Symp. on Improved Oil Recovery, Tulsa, 22- 26 April.

Fjelde, I. 2008. Sulphate in Rock Samples from Carbonate Reservoirs. SCA 2008-19. International Symp. of the Society of Core Analysts, Abu Dhabi, October 29- 3 November.

Hamon, G. 2004. Revisiting Ekofisk and Eldfisk Wettability. SPE 90014. SPE Annual Technical Conference and Exhibition, Houston, Texas, 26-29 September.

Kvæstad, A.H. 2011. CO_2-Foaming Agent Retention in Fractured Chalk Rock - Experiments and Simulations. MSc. Thesis, Faculty of Science and Technology, University of Stavanger.

Manrique, E.J. Muci, V.E. Gurfinkel, M.E. 2007. EOR Field Experiences in Carbonate Reservoirs in the United States. Paper SPE 10063. *SPE Res Eval & Eng* 10 (6): 667-686.

Morel, D., Bourbiax, B., Latil, M., Thielbot, B. 1993. Diffusion Effects in Gas Flooded Light-Oil Fractured Reservoirs. Paper SPE 20516. *SPE Advanced Technology Series 1* (2):100-109.

Rossen M. J. ed. 2004. Reduction of Surface and Interfacial Tension by Surfactants. In *Surfactants and Interfacial Phenomena*. 3rd Edition. New York: John Wiley and Sons, Incorporated. Chap. 5, 208-242.

Standnes, D.C. and Austad, T. 2000. Wettability Alteration in Chalk 2: Mechanisms for Wettability from Oil-Wet to Water-Wet using Surfactants. *J. Pet Science Eng*, *28*, 123-143.

Strand, S., Hjuler, M.L., Torsvik, R., Madland, M.V., and Austad, T. 2007. Wettability of Chalk: Impact of Silica, Clay Content and Mechanical Properties. *Petroleum Geosciences*, 13 (1): 69-80.

Schmitt T. M. 2001. Titration of Surfactants. In Analysis of Surfactants. Surfactant Science Series, 2nd edition. 96, Chap. 16, 490-493. New York: Marcel Dekker Incorporated.

Zuta, J., Fjelde, I., and Berenblyum, R, A. 2009. Oil Recovery during CO_2-Foam Injection in Fractured Water Flooded Chalk at Reservoir Conditions. Paper SCA-A27. International Symp. of the Society of Core Analysts, Noordwijk, The Netherlands, 26-30 September, 2009.

Zuta, J., Fjelde, I., and Berenblyum, R. 2010a. Experimental and simulation of CO_2-foam flooding in fractured chalk rock at reservoir conditions: Effect of mode of injection on oil recovery. Paper SPE 129575. SPE EOR Conf. at Oil & Gas West Asia, Muscat, Oman, 11-13 April.

Zuta, J., Fjelde, I., and Berenblyum, R. 2010b. Modeling Transport of a CO_2-foaming agent during CO2-foam processes in fractured chalk rock. Paper SPE 129601. SPE IOR Symp., Oklahoma, Tulsa, 26-28 April.

Ion	Formation water (FW) [mol/l]	Seawater (SW) [mol/l]
Na^+	629.844	439.188
K^+	4.158	10.060
Mg^{2+}	22.036	45.007
Ca^{2+}	226.166	12.992
Cl^-	1130.407	526.106
SO_4^{2-}	0.000	19.569
HCO_3^-	0.000	0.002

Table 1. Ionic compositions of synthetic FW and SW.

Fluid properties		FW	SW	Surfactant solution (0.86wt%)	Stock tank oil
Density	**[g/cc]**	1.00	1.01	1.02	0.82
Viscosity	**[cp]**	0.51	0.52	0.61	5.2
pH	**[pH units]**	7.4	8.2	8.2	-
IFT (with STO)	**[mN/m]**	-	28	3.0	-

Table 2. Density, viscosity, pH measurements of fluids at 1 atmospheric pressure and 55°C.

Plugs	Length [cm]	Porosity [%]	k_{abs} [mD]	Comments (see Figure 2)
AH16	7.01	40.2	0.63	No blockage
A22	7.02	40.0	0.71	No blockage
AH25	7.05	39.9	0.91	Lateral surface blocked
A26	7.04	39.8	0.92	Lateral surface blocked
A27	7.00	40.1	0.91	Bottom and half lateral surface blocked
A28	7.02	40.0	0.92	Bottom and half lateral surface blocked
A29	7.04	41.7	0.93	Lateral surface and top blocked
A31	7.08	41.6	0.92	Lateral surface and top blocked
A32	7.06	41.1	0.90	Lateral surface and bottom blocked
A33	7.08	42.2	0.91	Lateral surface and bottom blocked

Table 3. The properties of the core plugs at S_w = 100% used in fractured models.

Plugs	Length [cm]	Porosity [%]	k_{abs} [mD]	S_{wi} [%]	S_{orw} [%]	k_{ro} (S_{wi})	k_{rw} (S_{orw})	Comments (See Figure 2)
FB29	7.11	43.1	1.83	15.6	30.4	0.37	0.43	Lateral surface and bottom blocked
FB30	7.09	42.1	1.87	17.3	23.9	0.32	0.32	Lateral surface blocked

Table 4. The properties of the core plugs at S_{orw} used in fractured models.

Product	Saturation [%]	Retention (ADMAXT) [mg/g rock]	Retention (ADMAXT) [gmol/cm3]	ADMAXT Used [gmol/cm^3]	Diffusivity [cm^2/min]
ACG	100	1.36	1.26*10e-5	1.26*10e-5	3*10e-5
	S_{orw}	1.36	1.26*10e-5	1.26*10e-b	2.1-2.3*10e-5

Table 5 Measured, maximum adsorption capacity (ADMAXT) and diffusivity used at 55°C. The value of "b" were varied in order to find the best history-match in plugs with S_{orw}.

Residual adsorption level (ADRT)	0 mol/cm^3 PV
Accessible pore volume (PORFT)	1
Residual resistance factor (RRFT)	1

Table 6 Other unchanging (default) rock and fracture parameters used.

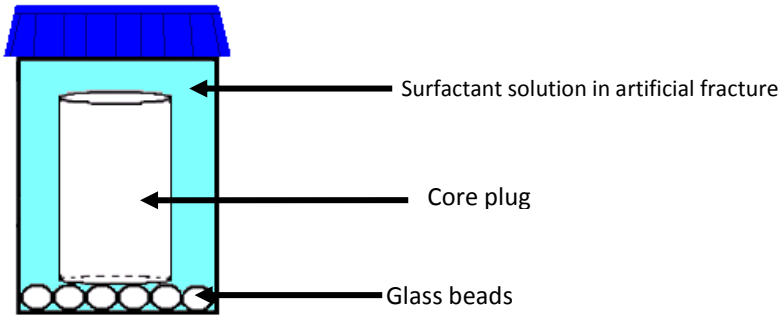

Figure 1. Sketch of the fractured model used in experiments.

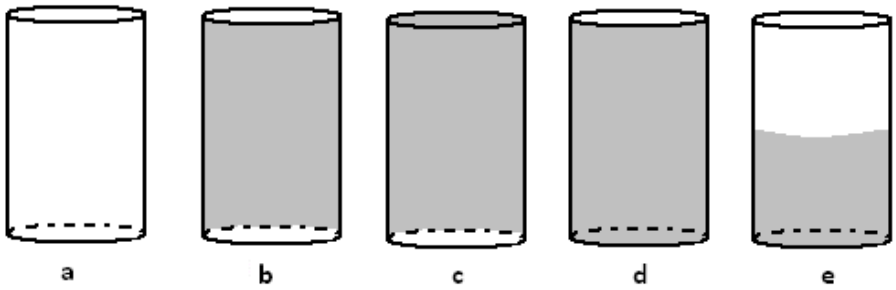

Figure 2. Sketches of different designs of fractured models. Grey shading shows blocked surface areas; a) No surface area blocked, b) Lateral surface area, c) Top and lateral surface area, d) Bottom and lateral surface area, e) Bottom and half of lateral surface area.

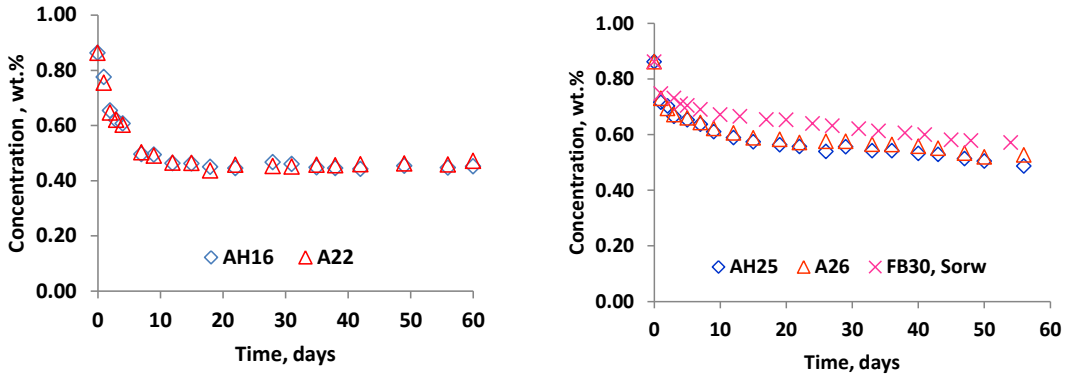

Figure 3. Surfactant concentration vs. time (a) base case experiments - two parallel core plugs with no surface area blocked at S_w=100% and (b) two parallel core plugs, AH25 and A26, with lateral surface area blocked at S_w = 100 %. Figure also shows profile for plug FB30 at S_{orw}.

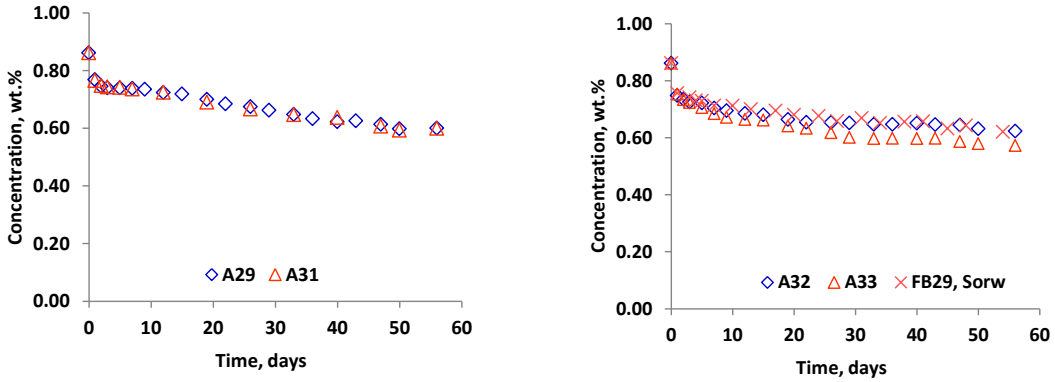

Figure 4: Surfactant concentration vs. time (a) two parallel core plugs, A29 and A31, with lateral surface area and top blocked (b) two parallel core plugs, A32 and A33 at S_w = 100% with lateral surface area and bottom blocked. Results for core plug at S_{orw}, FB29, with lateral surface area and bottom blocked also shown.

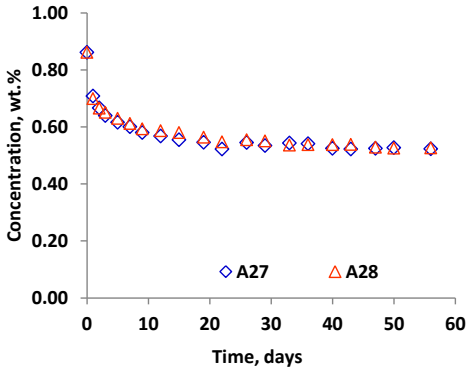

Figure 5: Surfactant concentration vs. time for two parallel plugs A27 and A28 with half of lateral surface area and bottom blocked at S_w = 100%.

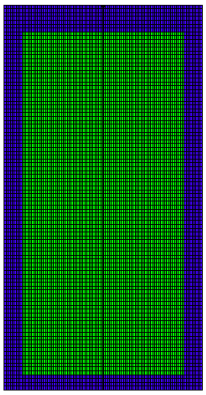

Figure 6. Grid of 50*1*100 grid blocks established in STARS. Blue area is artificial fracture and green area is core plug with either S_w = 100% or S_{orw}.

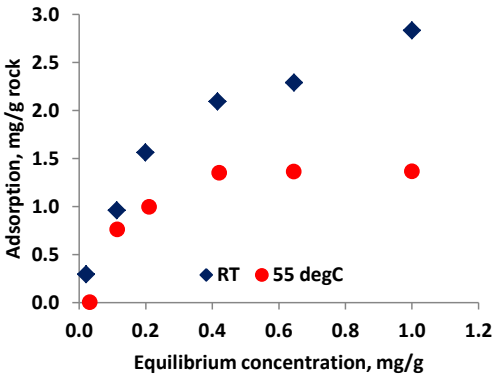

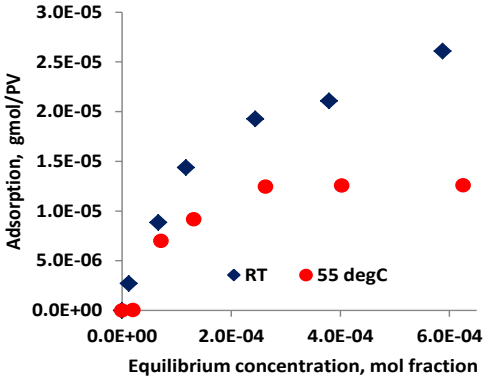

ɪ 55°C.

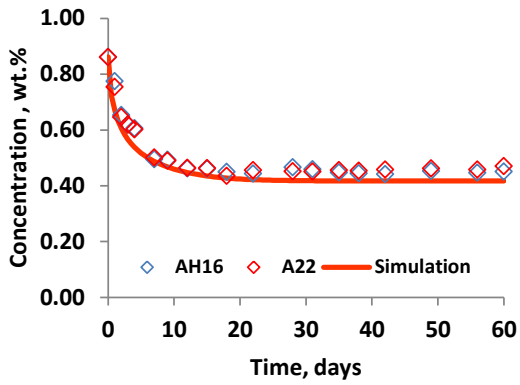

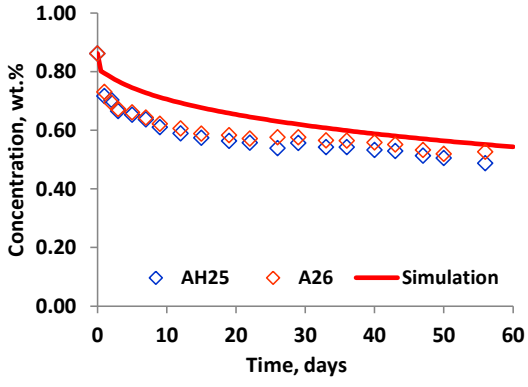

case experiments with no surface area blocked and (b) lateral surface area blocked for plugs AH25 and A26 at S_w = 100 %.

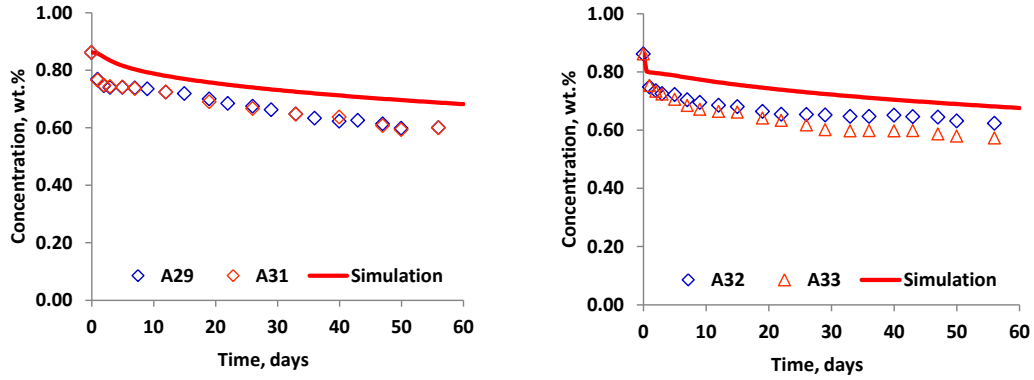

Figure 9: Surfactant concentration vs. time for experiments and prediction (a) lateral surface area and bottom blocked for plugs A32 and A33 at S_w = 100 %.

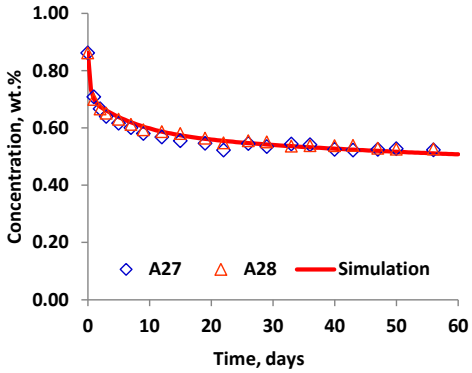

Figure 10: Experimental data and predicted in plugs A27 and A28 where half the lateral surface area

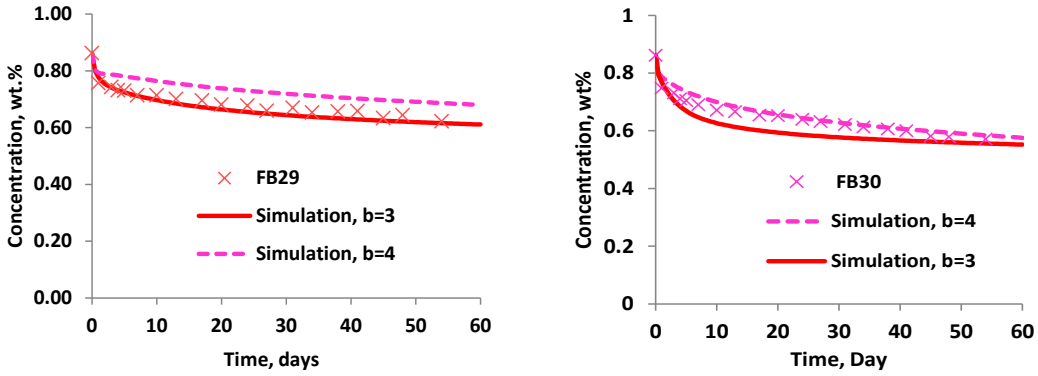

Figure 11: Surfactant concentration vs. time for experiment and different history-matches where (a) the lateral surface area and bottom blocked for plug FB29 (ADMAXT = $1.26*10^{-b}$ mol/cm^3 PV, where b = 3 or 4) (b) surfactant concentration vs. time for experiment and different history-matches where the lateral surface area blocked for FB30 at S_{orw} (ADMAXT = $1.26*10^{-b}$ mol/cm^3 PV, where b = 3 or 4).

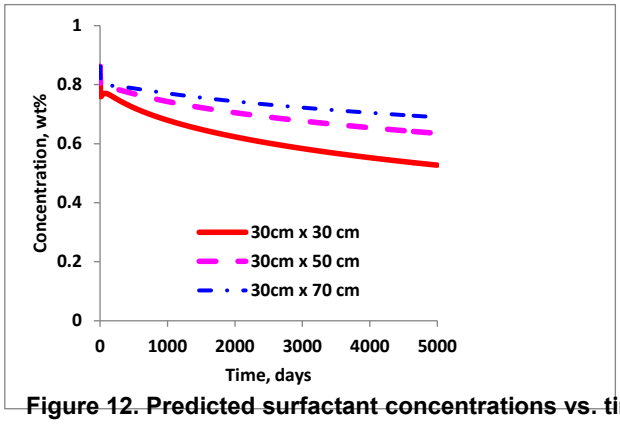

Figure 12. Predicted surfactant concentrations vs. time for large matrix blocks at S_w=100%.